

Seepage Behavior of Drainage Zoning in a Concrete Faced Gravel-fill Dam via Centrifuge and Numerical Modeling

Yun Wook Choo*, Dong Hoon Shin**, Sung Eun Cho***, Eun Sang Im****, and Dong-Soo Kim*****

Received July 25, 2011/Revised July 16, 2012/Accepted September 16, 2012

Abstract

Sandy gravel materials have recently been utilized in place of crushed rock materials as the main rockfill materials in Concrete Faced Rockfill Dams (CFRD) to address geological and environmental problems. In this paper, an experimental scheme for centrifuge modeling was developed to simulate a Concrete Faced Gravel-fill Dam (CFGD). The dam considered in this study was designed to implement a drainage zone of high permeability in the main gravel-fill zone to enhance safety against accidental water infiltration into the dam. Two centrifuge tests were performed and compared to investigate the performance of the drainage zone. The first test was done with the drainage zone and the second without the drainage zone. In the centrifuge tests, water infiltration was simulated by raising the water table over pre-implemented cracks on the model face slab. The infiltration behaviors were monitored by pore water pressure transducers. The centrifuge tests showed that the drainage zone of the CFGD effectively drains infiltrating water out of the dam body in a short time. Numerical modeling was also performed to help understand the process of seepage through cracks.

Keywords: concrete faced gravel-fill dam, centrifuge modeling, zoning, seepage, drainage zone

1. Introduction

A CFRD (Concrete Faced Rockfill Dam) is a widely used type of dam that prevents seepage flow into the dam body via a concrete face slab installed on the upstream slope. Even if water infiltrates into the dam due to damage to the face slab, the dam remains stable because the rockfill drains freely. This seepage control mechanism therefore does not allow pore water pressure buildup in the dam body. CFRDs provide numerous other advantages as well, including the possibility of using local materials, cost-effectiveness, extensive adaptability, simpler design and construction, shorter construction periods, and enhanced stability in the event of earthquakes (Xing *et al.*, 2006). Due to these advantages, many concrete faced rockfill dams have been and are being constructed globally. Nevertheless, considering the current state of technology, the design of CFRDs is based on previous practical and successful experience instead of design theories (Cooke, 1984).

Gravel-fill materials are often utilized in place of crushed rock materials as the main fill material in CFRDs. It is well known

that CFGDs (Concrete Faced Gravel-fill Dams) have advantages over CFRDs in terms of environmental and economical aspects. The gravel-fill materials have strength and deformation properties that are comparable to those of rock-fill material in existing stable CFRDs. Therefore, a CFGD is often considered to be a feasible solution if the construction site is rich with gravel deposits.

The water barrier system of a CFRD or a CFGD is not permanently waterproof; hence, the possibility exists of water infiltration through the damaged face slab caused by structural flaws, aging, and earthquake loading. Accidental infiltration requires additional consideration of seepage control. In general, the permeability of rockfill is so high that it is considered to be a stable material for seepage problems. However, sandy gravel fill has a low permeability coefficient of 10^{-4} to 10^{-5} m/s and segregates easily during the construction process. This segregation leads to stratification in the dam, resulting in much smaller vertical permeability compared to horizontal permeability. Therefore, a sandy gravel fill dam requires a secondary measure to control water flow through establishment of a drainage path in the zone

*Member, Research Professor, Dept. of Civil and Environmental Engineering, Korea Advanced Institute of Science and Technology (KAIST), Daejeon 305-701, Korea (E-mail: ywchoo@kaist.ac.kr)

**Member, Head Researcher, K-water Institute, Korea Water Resources Corporation, Daejeon 305-730, Korea (E-mail: jiban.shin@gmail.com)

***Member, Assistant Professor, Dept. of Civil, Safety and Environmental Engineering, Hankyong National University, Anseong 456-749, Korea (Corresponding Author, E-mail: drsecho@hanmail.net)

****Senior Researcher, K-water Institute, Korea Water Resources Corporation, Daejeon 305-730, Korea (E-mail: esim89@kwater.or.kr)

*****Member, Professor, Dept. of Civil and Environmental Engineering, Korea Advanced Institute of Science and Technology (KAIST), Daejeon 305-701, Korea (E-mail: dskim@kaist.ac.kr)

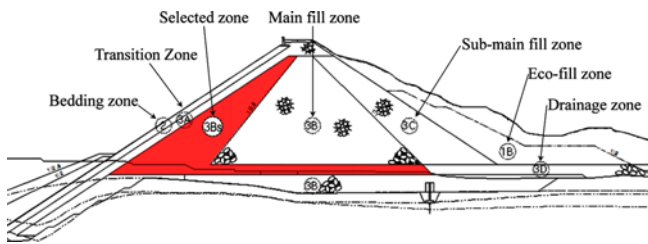


Fig. 1. Schematic Design Layout of the CFGD in This Study

layout of the dam. Thus, in the design of a dam, the emphasis of the design should be placed not only on deformation control but also seepage control of the dam. For the design of a concrete face gravel fill dam, seepage control has become a main design concern (Wang and Qu, 2000). Although many studies on the deformation characteristics of CFRDs have been carried out (Clements, 1984; Hunter and Fell, 2003; Seo *et al.*, 2009), seepage behavior is still not well understood.

In this paper, a case involving the seepage control design of a CFGD is investigated through centrifuge and numerical modeling. The CFGD is located on a tributary of the Gamchun stream in mid-southern Korea. The CFGD is 64 m high and 472 m long. It has a total storage capacity of 54.27 million m^3 . The rockfill and gravel fill volume of the dam body is close to 2.16 million m^3 . This CFGD was designed to implement Zone 3Bs for drainage purposes in front of the main fill Zone 3B, as shown in Fig. 1. Zone 3Bs has much higher permeability compared to the main gravel-fill zone (3B), thereby enhancing seepage stability against unexpected water infiltration. The dam was designed with gravel-fill as the main fill material because sand and gravel fill materials can be easily supplied near the dam site along the main stream. In order to investigate the seepage control performance of the dam, an experimental scheme of centrifuge modeling for simulating the CFGD was developed. In order to investigate the effect of Zone 3Bs on the seepage flow, two centrifuge tests were carried out on two models with different zone layouts: one designed without Zone 3Bs and one with Zone 3Bs. Water infiltration was simulated by raising the water table over pre-implemented cracks on the model face slab. The centrifuge test results were then compared and analyzed considering seepage flow through the drainage zone.

2. Damage of Concrete Face Slab

Gouhou dam in China is a typical example of a CFRD that failed by seepage caused from concrete face slab damage. In 1993, the Gouhou dam failed during impounding due to water infiltration into the dam through a joint between the bottom platform of a parapet wall and the concrete face. Many studies on the failure of the Gouhou dam have been carried out (Liu and Miao, 1996; Chen and Zhang, 2006; Zhang and Chen, 2006). Chen and Zhang (2006) and Zhang and Chen (2006) studied the stability of the dam using a saturated-unsaturated seepage analysis. They concluded that one of the most probable causes of

the failure was stratification due to the segregation of soil particles during construction. Stratification may have caused the horizontal spreading of water infiltration in the middle of the dam, which may have then flowed out of the downstream slope at a high elevation, resulting in the final failure.

Damage of the concrete face slab is mainly caused by bending or compressive stresses which are induced by differential settlement or excessive deformation of the dam body. Such deformations may be caused by the time-dependent characteristics of the construction material, by the water load during impounding, or by dynamic loadings such as earthquakes. In addition, separation of the concrete face slab from the cushion layer is inevitable due to the differential settlement or deformation of the dam body and the concrete slabs (Cooke, 1984).

Extensive rupturing of the concrete face under compression occurred at the Campos Novos dam in Brazil in October of 2005 (Pinto, 2008; Xavier *et al.*, 2008). Initial impoundment created significant transversal deformations of the rockfill embankment and, in turn, increased high compressive stresses in the center of the concrete slab, resulting in rupture of the slab. Similar observations were also reported at the Mohale dam in Lesotho in February of 2006 and in the Barra Grande dam in September of 2006. In all three cases, the extent of damage was significant and the cracks produced sudden and noticeable leakage into the dam body (Pinto, 2008). These developments drew attention to a phenomenon that had previously been undetected. It was discovered that high compressive strains could be imposed on concrete face slabs due to an adverse combination of dam height, low rockfill deformation modulus and unfavorable valley shape. These accidents of the face slab did not result in total failure of the dams because immediate measures, pouring silt and fine sand over the slabs and lowering the upstream water level, were taken. Nevertheless, these cases emphasize that extensive rupturing of the concrete face and water leakage can occur at any time.

3. Centrifuge Modeling of CFGD

3.1 Design of Centrifuge Models

Understanding the behavior of a CFGD is critical for both design and safety evaluation. Therefore, the behavior should be estimated realistically in both the construction and reservoir filling stages. Centrifuge tests are one of the tools available to predict the mechanical behavior of an earth structure, as centrifuge modeling can physically simulate the in-situ stress level inside the earth material of the model. Centrifuge tests must satisfy all the laws of similitude to the greatest extent possible and simulation of the construction materials is a key procedure in centrifuge tests for a CFGD.

In this paper, two centrifuge tests were designed to distinguish the effects of zoning by different zone layouts. One (termed CASE I) excluded a drainage zone (denominated as Zone 3Bs) from the prototype design; the other (termed CASE II) included a drainage zone (Zone 3Bs). The model CFGD consisted of four zones: Zone 3B (the main-fill), Zone 2 (the bedding zone), Zone

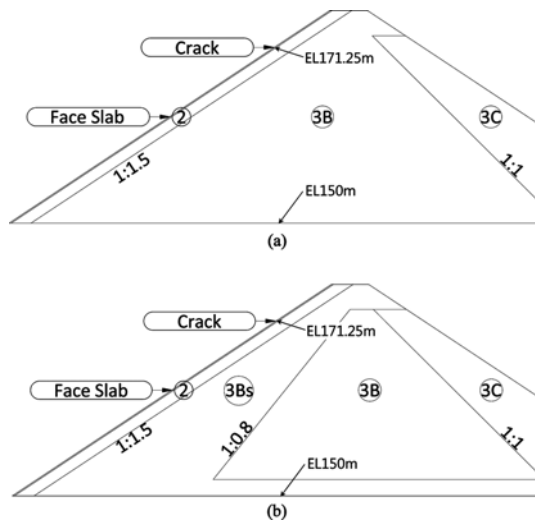


Fig. 2. Cross-sections of Centrifuge Models: (a) CASE I, (b) CASE II

3Bs (the selected zone for drainage), and Zone 3C (the sub main-fill zone). Zone 3A, a filter zone to prevent loss of Zone 2 material, was simplified by using a geotextile for efficient model construction. The upstream blanket zone, the environment-friendly zone, the plinth and the parapet wall were not included in the model dams for simplicity. Final model cross-sections are presented in Fig. 2. A scaling ratio (N) of 60 (referring to the centrifuge acceleration) was selected. The height of the dam is 0.42 m in model scale (25 m in prototype). The prototypes of the models were intended to model half the size of the actual dam. The bottom level of the dam is defined as EL (elevation) 150 m as a datum. Cracks are implemented at EL171.25 m.

In centrifuge tests, researchers prefer to use the actual prototype soil in order to properly replicate its behavior. Dam material with large size particles could not be used in the centrifuge model due to the limitation of model size, making it necessary to reduce the grain size of the model dam material. For instance, the maximum particle size of the prototype Zone 3B and 3Bs is 500 mm; that of Zone 2 is 75 mm; and that of 3C is 800 mm. In the current state of technology, it is difficult to satisfy all the laws of similitude in a model test properly. A method to reduce the actual rockfill grain size to correspond with the model rockfill grain size for model preparation requires further study. Therefore, this study aims to investigate generic seepage behavior of a CFGD adopting a drainage system based on the design of an existing dam.

The grain sizes of dam materials were reduced by combination of the SPDM (Similar Particle Distribution Method) and the EQRM (Equal Quantity Replacing Method) (Xu *et al.*, 2006; Seo *et al.*, 2009). Fig. 3 shows the grain size distribution of the prototype and model materials. Fig. 4 shows the model materials prepared for centrifuge tests.

As a consequence of the change in the grain size distribution of the model material, the properties of the model material were changed and in-situ permeability coefficients could not be

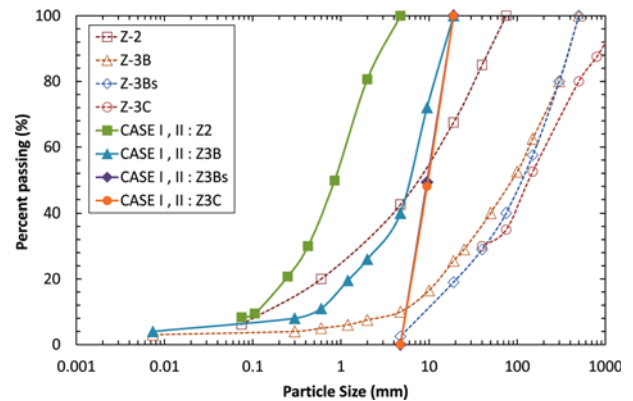


Fig. 3. Particle Size Distributions of Prototype and Model Materials



Fig. 4. Model Materials for Centrifuge Tests



Fig. 5. In-situ Permeability Tests

achieved with the treated model materials. Therefore, alternatively, the ratio between the permeability coefficients of the neighboring zones ($k_{\text{model}}/k_{\text{model}}$ for Zone 3B) was controlled to replicate that of the prototype permeability coefficients ($k_{\text{in-situ}}/k_{\text{in-situ}}$ for Zone 3B). First, the

Table 1. In-situ Permeability Coefficients of the Prototype Dam

Zone	In-situ permeability coefficient, $k_{in-situ}$ (m/s)	$k_{in-situ}/k_{in-situ}$ for Zone 3B *
Zone 2	1.0×10^{-6}	0.08
Zone 3B	1.23×10^{-5}	1
Zone 3Bs	2.34×10^{-4}	19

* $k_{in-situ}$ = in-situ permeability coefficient; $k_{in-situ}$ for Zone 3B = in-situ permeability coefficient for Zone 3B



Fig. 6. Large Scale Triaxial Shear Apparatus for Permeability Tests

Table 2. Permeability Coefficients of Model Dams

Zone	Permeability coefficient, k_{model} (m/s)	k_{model}/k_{model} for Zone 3B *	Compacted dry unit weight (kN/m ³)
Zone 2	9.85×10^{-8}	0.02	20.4
Zone 3B	6.44×10^{-6}	1	19.7
Zone 3Bs	1.36×10^{-4}	21	18.1

* k_{model} = permeability coefficient of model material; k_{model} for Zone 3B = permeability coefficient model material for Zone 3B

Table 3. Final Dry Unit Weight of Model Zones

Zone	CASE I (kN/m ³)	CASE II (kN/m ³)
Zone 2	20.4	20.4
Zone 3B	19.7	19.4
Zone 3Bs	-	18.1
Zone 3C	17.7	18.2

permeability coefficients of the prototype dam were measured by in-situ permeability tests. The in-situ tests were performed during construction (Fig. 5) and the permeabilities of the prototype dam are tabulated in Table 1. In addition, the permeability coefficients of the model materials at different compaction densities were measured by using a large scale triaxial shear testing apparatus capable of handling 300 mm diameter specimens (Fig. 6 and Table 2). Based on the relationship between the permeability coefficient and density, the permeability coefficients for the model dams were controlled. The final compaction conditions of each model zone are listed in Table 3.

Regarding the model face slab, it was impossible to model the bending stiffness of the prototype concrete face properly using concrete; thus, an aluminum plate was used for the models. The thickness of each layer of the aluminum plate was determined

Table 4. Specifications of Geotechnical Centrifuge at KAIST

Items	Specifications
Manufacturer	Actidyn Systems Inc.
Platform radius (m)	5.0
Maximum capacity	240 g-tons
Maximum acceleration	130 g
Maximum payloads	2,400 kg (up to 100 g)
Size of Container	1.2 m(L) × 1.2 m(W) × 1.2 m(H)

using Eq. (1) (Schofield, 1980; Taylor, 1995).

$$E_m I_m = \frac{(EI)_p}{N^3} \quad (1)$$

Here, E = the elastic modulus (F/L²); I = the moment of inertia per unit width (L⁴/L); EI = the bending stiffness per unit width (F·L²/L); N = a scaling factor; m = the model; and p = the prototype. The Young's moduli for concrete and aluminum were assumed to be 28 GPa and 70 GPa, respectively. The thickness of the prototype face slab was assumed to be 0.15 m. Based on the dimensions and modulus, the required model plate thickness was 1.84 mm. A thickness of 2.0 mm was selected for the tests.

3.2 Model Construction and Testing Procedure

Centrifuge tests were performed using the 240 g-ton geotechnical centrifuge equipment at KAIST (Korea Advanced Institute of Science and Technology) in South Korea. Table 4 shows the specifications of the KAIST geotechnical centrifuge and detailed information of the centrifuge can be found in Kim *et al.* (2013).

Model dams were constructed with eight layers. Each layer was compacted separately with wooden blocks to hold the designed slope and density constant during compaction. The construction procedure is shown in Fig. 7. After the construction

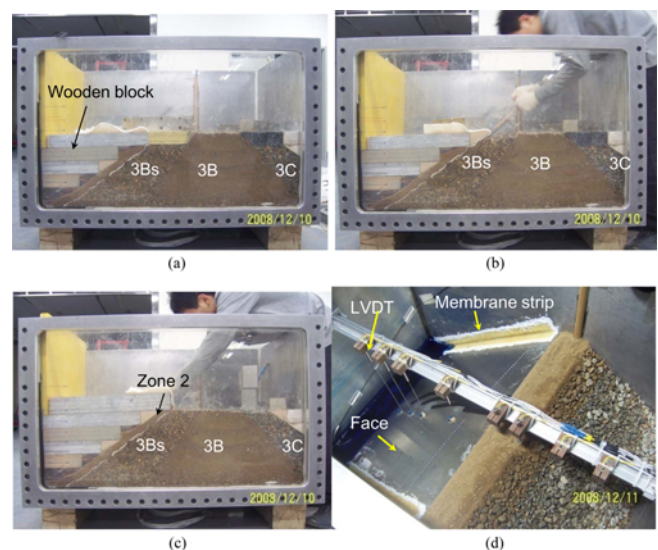


Fig. 7. Construction Procedure of Centrifuge Models: (a) Compaction of Zone 3B, (b) Compaction of Zone 3Bs, (c) Compaction of Zone 2, (d) Completion of Model Dam

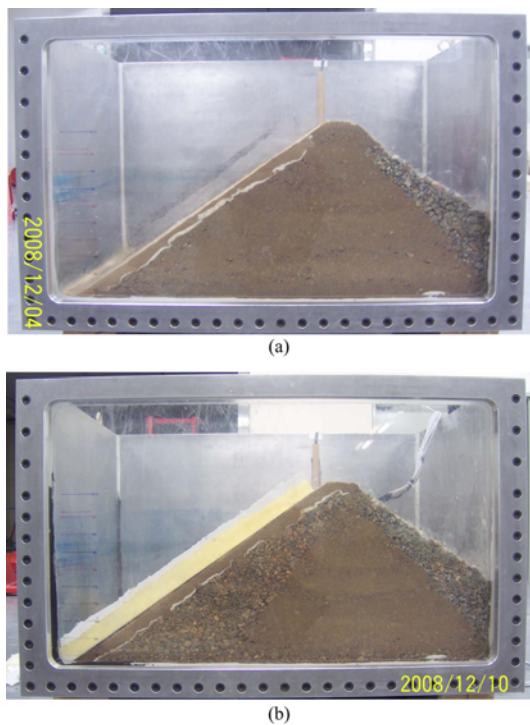


Fig. 8. Pictures of Completed Models: (a) CASE I, (b) CASE II

of the model dam, the model face slab was placed on the upstream slope of the model dam. The boundary of the model face was bound to the model container wall by latex membrane strips and the latex membrane strips were glued with silicone paste. This binding provides free movement of the face and prevents leakage through the gap between the face and the model container wall. Fig. 8 shows images of CASE I and CASE II as completed. After preparation of the model dam, water was filled slightly in the upstream side and dyed with aqueous paint to highlight seepage flow during the simulations. The flow of the colored water was recorded using an analog camera installed at the window side of the model container.

In order to simulate accidental water infiltration through cracks across the face slab, holes were made on the model face slab at pre-determined locations (EL171.25 m). Water was remotely supplied to the upstream through a solenoid valve connected on a wall on the upstream side. During the spin of the centrifuge, the water table was raised over the pre-implemented holes to provide water infiltration into the dam body. In order to place a free outlet boundary on the downstream, drainage holes were implemented on the downstream-side wall, as depicted in Fig. 9. This allows the arrived water to discharge immediately at the downstream boundary.

To monitor the behavior of the model, three types of sensors were used, as shown in Fig. 9. L1 to L8 denote LVDTs, which measured the vertical settlement of the dam surface. S1 to S8 represent the strain gages on the surface of the model face that measured surface stress during impoundment and water infiltration. P1 to P5 are pore water pressure transducers. P1 is

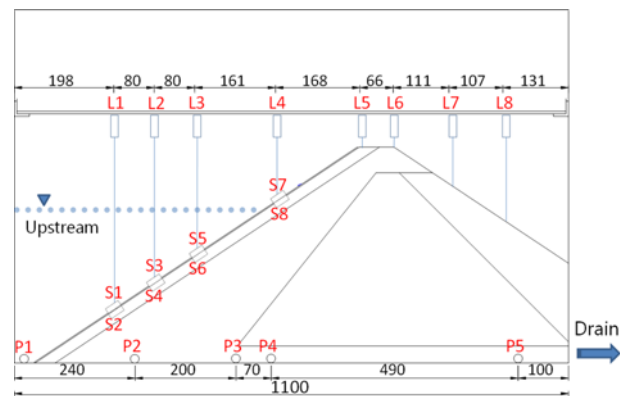


Fig. 9. Layout of Instrumented Sensors

used to monitor the upstream water level. P2 to P5 were buried underneath the model dam from upstream to downstream to measure the accumulated pore water pressure inside the dam.

4. Centrifuge Test Results and Discussion

The measured pore water pressure after the water infiltration started is plotted in Fig. 10. P3 measures slightly higher pore water pressure at 80 seconds than the others, which is a result of the infiltrated water dropping onto and accumulating at P3. On

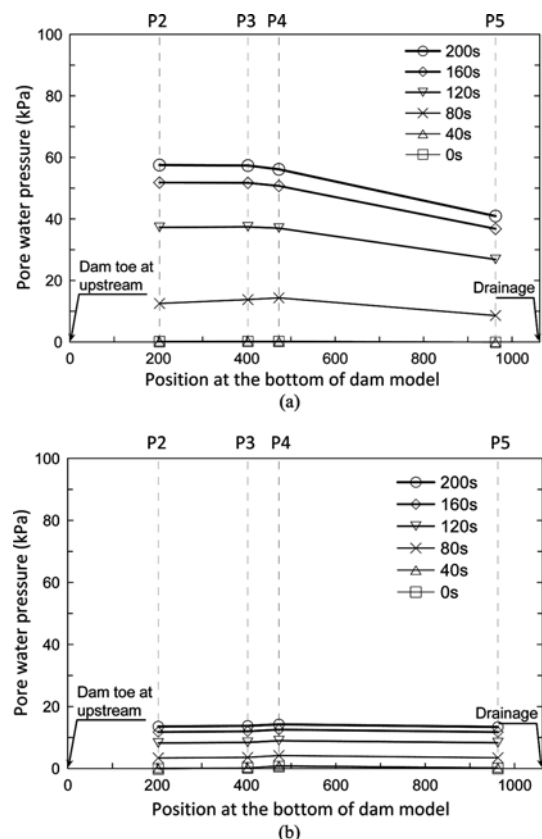


Fig. 10. Pore Water Pressure Distributions during Infiltration (In Model Time Scale): (a) CASE I, (b) CASE II

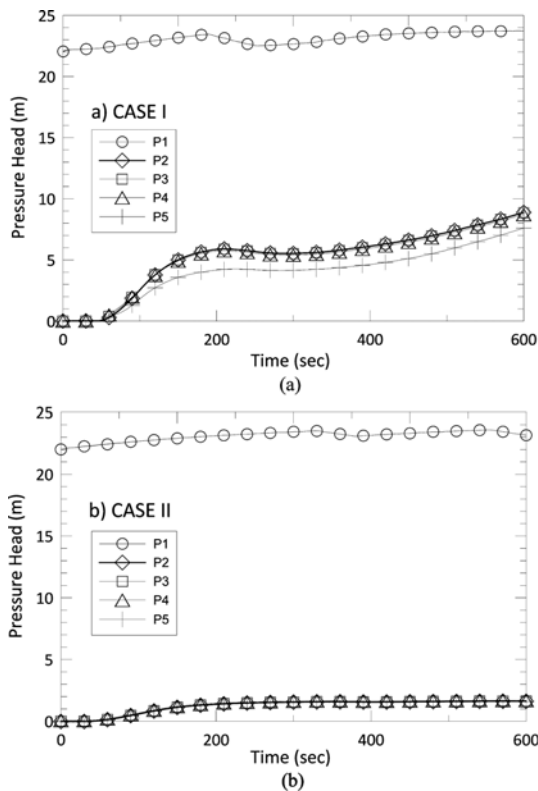


Fig. 11. Time History of Pore Water Pressure Head at Measuring Points (In Model Time Scale): (a) CASE I, (b) CASE II

the other hand, higher pressure of P3 was not observed in CASE II, because the drainage of 3Bs was much faster than the accumulation from the cracks. In addition, interestingly, the pore water pressure level of CASE II converged to a pressure value that corresponds to the thickness of the bottom drainage layer in approximately 200 seconds, while that of CASE I continued to increase at the same time. It can be concluded that the drainage zone (Zone 3Bs) in CASE II successfully discharged the infiltrated water.

Figure 11 shows the time history of the pore water pressure collected at the measuring points of the centrifuge tests (P1 to P5). For CASE I, it was expected that the pore water pressures would increase at different rates, because the pore water pressure sensors are located at different distances from the water infiltration holes. This is inferred from a numerical simulation described in the next section. However, in the centrifuge tests, most of the sensors (P1 to P4) increase at similar rates, because seepage flow in the centrifuge tests might be accelerated by the high permeable boundaries of the construction joints created in Zone 2 and those between the model dam and the container walls. In addition, it is noted that the accumulated water increased at the end of the test because Zone 3B was not permeable enough to drain the water off. Fig. 11(b) plots variations in the pore water pressures for CASE II. All pressures started to increase almost simultaneously because the infiltrating water flew quickly through Zone 3Bs. It is noteworthy that the pressure heads of all

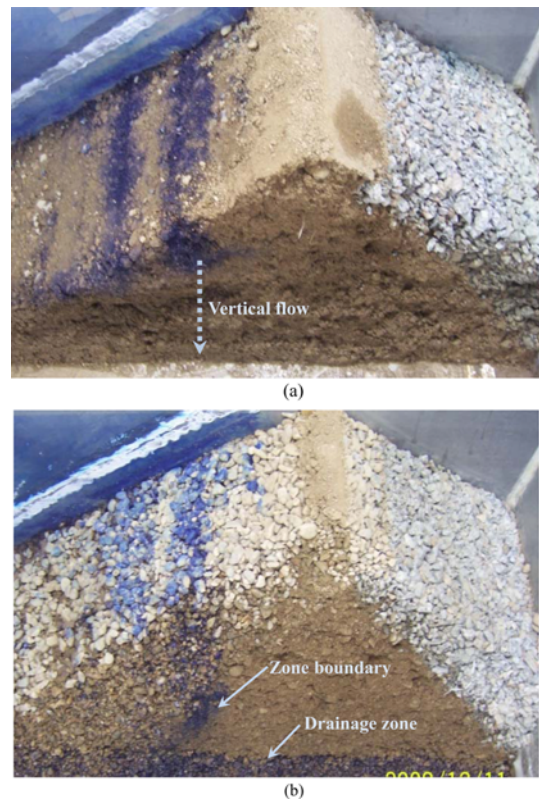


Fig. 12. Observation after Excavation: (a) CASE I, (b) CASE II

pressure sensors converged to the height of the horizontal layer in Zone 3Bs.

After the centrifuge tests, the models were excavated to trace the water flow, as shown in Fig. 12. In CASE I, it was observed that a vertical water trace was left behind from the cracks to the bottom, showing that the infiltrating water flew vertically through the unsaturated fill of the dam. Similarly, in CASE II, the vertical water trace was found from the cracks at the beginning of the water infiltration. However, the flow path turned left when the water faced the interface between Zone 3B and 3Bs, following the boundary slope of Zone 3Bs. This water trace continued to the horizontal Zone 3Bs passage (horizontal drainage) layered below Zone 3B, as shown in Fig. 12(b). This result is consistent with the pore pressure results and supports the aforementioned conclusion.

Based on the results of this study, the vertical part of Zone 3Bs (vertical drainage) mainly collected the water infiltrated through the face slab; the infiltrated water was then drained away from the dam body through horizontal drainage. The horizontal drainage also collected the water that infiltrated from Zone 3B (although the amount of water was not significant) and transferred it downstream of the dam. Face slab cracks can appear at any position of the face slab. Therefore, the vertical drainage mechanism must be built through the entire cross-section (perpendicular to the river valley) to cut off all water that infiltrates through the seepage prevention lines in the dam body and to prevent water from leaking downstream of the dam body (Wang and Qu,

2000).

In addition, it is important to note that a distinct water trace remained on several locations of Zone 2, distributed in the transverse direction. This localized water passage formed on construction joints stratified between the compacting layers; the local passage accelerated the seepage flow through Zone 2. Zone 2 is designed as a very low permeable layer because it is supposed to reduce the water flow rate. Hence, it is probable that the possible construction joints undermine the original function of Zone 2, emphasizing the importance of quality control during the construction process as well as the secondary seepage control design (Zone 3Bs).

5. Numerical Simulation

5.1 Numerical Modeling and Boundary Conditions

In order to help understand the process of seepage through cracks, a numerical simulation was conducted on the same prototype as used in the centrifuge test. Most of the zone materials were initially dry or unsaturated because water flow was prevented by the face slab. Thus, saturated-unsaturated seepage theory was used to analyze water infiltration into the dam body. The numerical simulation was conducted using SEEP/W, a commercial finite element program to investigate the propagation of the wetting front and the distribution of the pore water pressure. The numerical simulation modeled the prototype section of the centrifuge tests with the soil properties tabulated in Table 2.

According to observations after excavation of the centrifuge model, as previously shown in Fig. 12, the water spread over the region in which the separation between the face slab and the Zone 2 material appeared. Therefore, it is assumed that the upstream face slab is ineffective from EL 167 m to EL 171.25 m and that a total head condition was imposed on this region. The boundary condition on the remaining part of the upstream slope is a zero flux condition, simulating an impermeable face. On the downstream side, it is assumed that the boundary of the downstream slope from EL 151 m to 151.5 m is defined as a zero flux condition if the total head is less than the elevation head; thus a free outlet boundary to simulate the drainage condition in the centrifuge model was assumed. The initial water level in the dam was assumed to be at EL 150 m (at the bottom of the model in the centrifuge model). Above the initial water table, the initial suction head increases linearly with the elevation; the maximum suction head is limited to 1 m because actual suction was unobtainable.

A transient seepage analysis of saturated-unsaturated soils requires two soil property functions: the soil-water characteristic curve and the permeability function. The soil-water characteristic curve represents the relationship between the volumetric water content and the matric suction in the soil. The four materials of the centrifuge model consist of large grains, which make it difficult to obtain the soil property curves by experimental work. In this study, the soil-water characteristic curves were

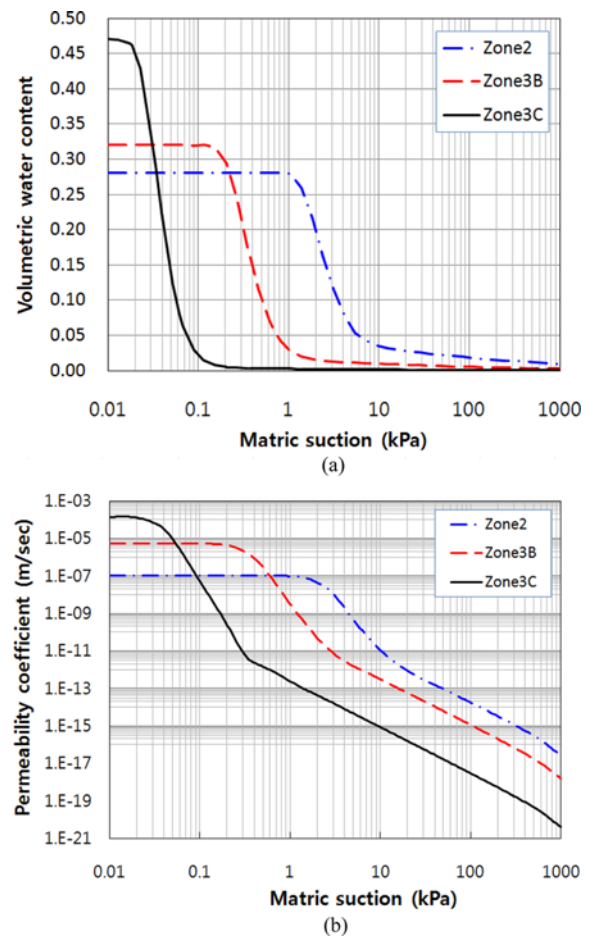


Fig. 13. Estimated Hydraulic Properties: (a) Soil-water Characteristic Curves, (b) Permeability Curves

estimated from the grain size distribution and basic soil properties using the modified Kovacs method (Aubertin *et al.*, 2003), which was implemented in SEEP/W, as shown in Fig. 13(a). The permeability of unsaturated soils is not constant but is influenced by the volumetric water content related to the matric suction. The permeability curves were estimated from the soil-water characteristic curve. The saturated permeability was estimated using the Fredlund method (Fredlund *et al.*, 1994), as shown in Fig. 13(b).

The estimated soil-water characteristic curves and permeability curves show a considerable amount of variation because the model materials consist of coarse grains that are less capable of retaining water. The steep curves may lead to a convergence problem. In this study, therefore, a transient analysis with adaptive time stepping was conducted to overcome the convergence problem.

5.2 Seepage Flow of CASE I without a Drainage Zone

The transient process of water infiltration of the case without Zone 3Bs, CASE I, was analyzed. The analysis was performed for three different values of permeability in Zone 2 for the same time duration.

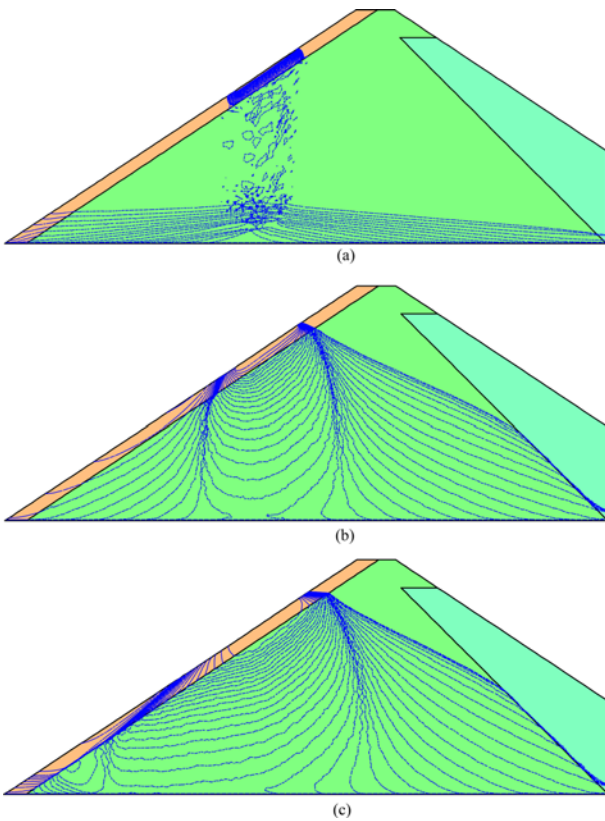


Fig. 14. Distributions of Water Front with Time during Infiltration Process for CASE I: (a) $k_{Zone\ 2} (=9.85 \times 10^{-8} \text{ m/s}) < k_{Zone\ 3B}$, (b) $k_{Zone\ 2} (=5.0 \times 10^{-6} \text{ m/s}) = k_{Zone\ 3B}$, (c) $k_{Zone\ 2} (=5.0 \times 10^{-5} \text{ m/s}) > k_{Zone\ 3B}$

Figure 14(a) shows the results obtained from the condition of Zone 2 being less permeable than Zone 3B. The figure shows the distributions of the wetting front, the contour for the zero pore water pressure, showing the advancement of the saturated zone due to infiltration of the water through the crack. Initially, the water gradually infiltrated into Zone 2 from the crack region initially. It took a long time for water to reach Zone 3B because the permeability of Zone 2 is very low. The infiltrating water moved through Zone 3B, whose permeability is much higher than that of Zone 2. With time, the water flow propagated vertically due to gravity. When the wetting front arrived at the bottom of the dam, the infiltrating water spread out in both the upstream and downstream directions. Since the upstream side was closed by the face, the water level rose over time.

When the permeability of Zone 2 is equal to that of Zone 3B, the amount of infiltrated water increases and the saturated zone in Zone 3B expands more quickly, as shown in Fig. 14(b).

If the permeability of Zone 2 becomes greater than that of Zone 3B (Fig. 14(c)), the seepage behavior in the dam is governed by Zone 3B. The wetting front infiltrated downward. In addition, under the condition of permeable Zone 2, the infiltrated water through crack can move downward following the interface between Zone 2 and Zone 3B due to the delay of water infiltration by the less permeable Zone 3B. Therefore, the

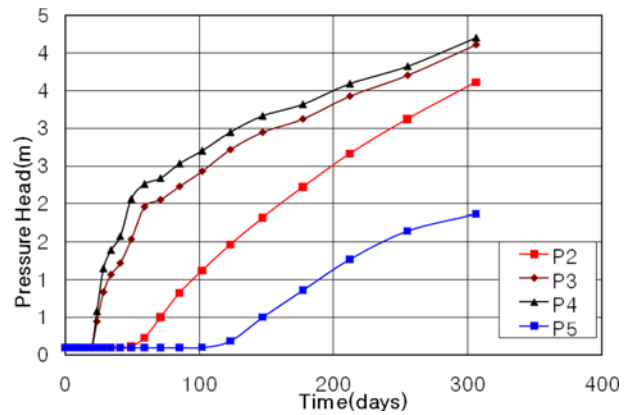


Fig. 15. Pore Water Pressure Head during Infiltration Process for CASE I with Less Permeable Zone 2 ($k_{Zone\ 2} = 9.85 \times 10^{-8} \text{ m/s}$)

wetting front propagated from the upstream to downstream direction.

The relatively less permeable Zone 2 limited the water flow and only a small amount of water infiltrated over a long time (Fig. 14(a)). If this does not occur, the amount of infiltrated water becomes large and the rising rate of the water level increases (Fig. 14(b) and Fig. 14(c)). The permeability of Zone 2 controls the seepage characteristics and the amount of water that infiltrates into the dam. Therefore, during construction, quality control should be heeded to achieve design permeability. However, as was observed in the excavation of the model dams, most of the water flowed through the construction joints stratified between the compacting layers, providing a realistic representation of actual dam conditions. Thus, it was concluded that the design of a drainage zone inside the main fill area is a crucial secondary measure to protect a concrete faced dam.

In CASE I, the water level increased continuously, as did the pore water pressure. When the accumulated water reached Zone 3C, the water exited from the toe of the downstream slope, as shown in Fig. 14.

Figure 15 shows the time history of the pore water pressure in the numerical simulation for the condition of Zone 2 being less permeable than Zone 3B, collected at the measuring points of the centrifuge tests. Since the infiltrating water arrives directly at P3 and P4, the pore water pressures at P3 and P4 increase considerably; however, the pressures of P2 and P5 gradually increase because the flow distance is longer.

5.3 Seepage Flow of Case II with Drainage Zone

Figure 16 shows the results of CASE II, which had a drainage zone (Zone 3Bs). In this analysis, the seepage outlet in the Zone 2 layer is assumed to be free, by specifying drainage boundary conditions. Only Zone 2 is considered in the numerical analysis, since the drainage zone has such high hydraulic conductivity that it does not contribute to dissipation of the head loss. Fig. 16(a) shows the total head contours and flow paths at a steady state and Fig. 16(b) shows the pore water pressure head contours and flow

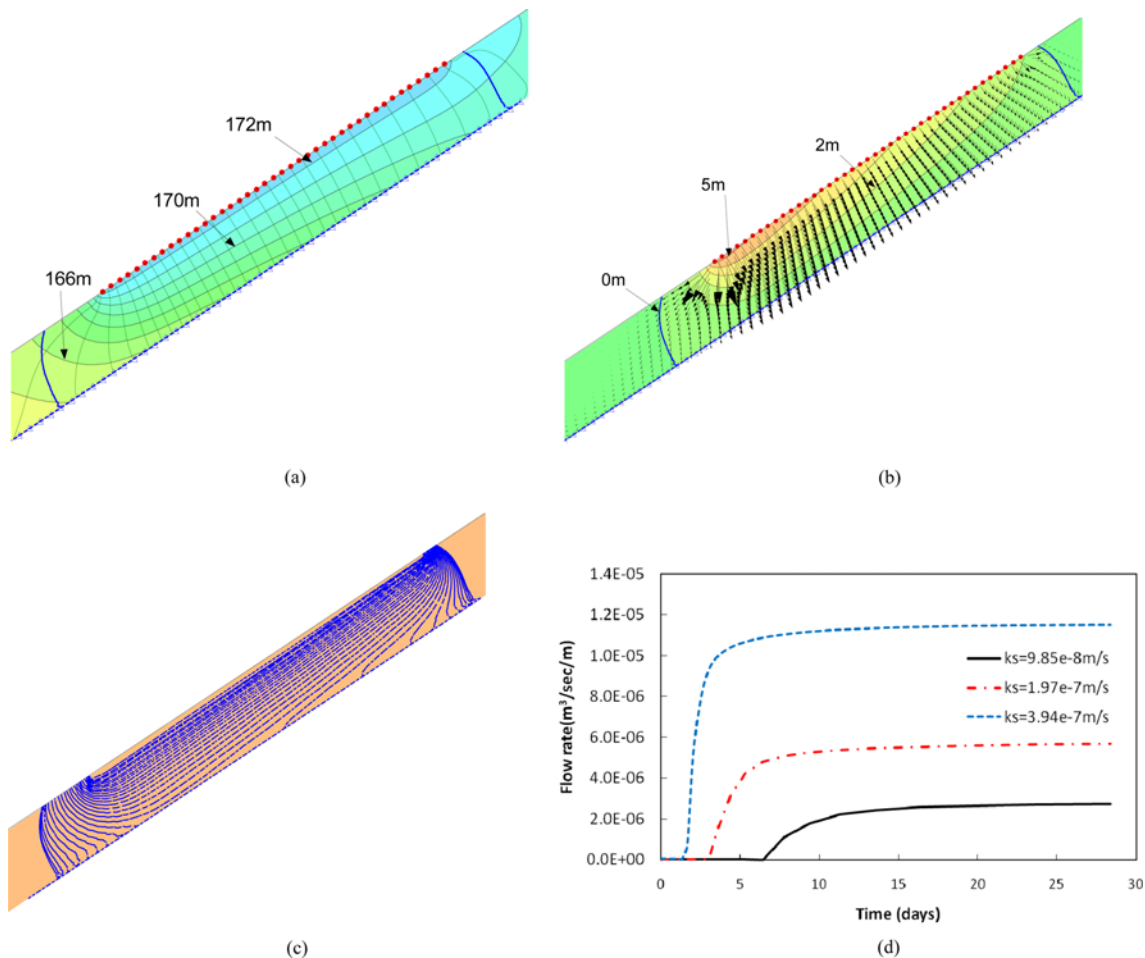


Fig. 16. Seepage Analysis Results for CASE II: (a) Total Head Contours and Flow Paths at Steady State, (b) Pore Water Pressure Head Contours and Flow Vectors at Steady State, (c) Distributions of Water Front with Time, (d) Total Outflow from Zone 2 with Time

vectors at a steady state. Seepage flow spreads sharply in Zone 2 after it passes through the crack. Large hydraulic head loss and a seepage gradient occur in the Zone 2. The flow pattern of CASE II was identical to that of CASE I before the wetting front arrived at Zone 3Bs.

Figure 16(c) shows the distribution of the wetting front that expands towards Zone 3Bs with time. Fig. 16(d) plots variations in the total seepage outflow from Zone 2. The figure shows that the total outflow rate increases with the increase of permeability in Zone 2, as the amount of seepage at steady state is directly proportional to the permeability. In addition, if the permeability in Zone 2 increases, the time to reach the steady state becomes shorter. The outflow water from Zone 2 will enter Zone 3Bs, and will move vertically through 3Bs. Subsequently, the accumulated water from the vertical part of Zone 3Bs (vertical drainage) will drain out through the horizontal layer of Zone 3Bs. The drainage system should thus apparently be designed to have sufficient capacity to discharge the amount of inflow from Zone 2. This theory is consistent with the results of centrifuge tests for CASE II showing that the drainage system successfully discharged all of the inflow water from Zone 2. The toe of Zone 3B also

becomes saturated over time and, eventually, the water level will stabilize to a steady state.

6. Conclusions

The purpose of this study was to analyze the seepage behavior in a CFGD by centrifuge modeling and numerical modeling when unexpected cracks are introduced on the concrete face slab. For this purpose, an experimental scheme for the centrifuge modeling of a concrete faced gravel-fill dam was developed. Two centrifuge tests were then performed to investigate the effects of drainage zoning on the seepage flow. The dam considered in this study was designed to have a Zone 3Bs (drainage zone) of high permeability in the main gravel-fill zone to enhance safety against accidental water infiltration into the dam.

The results of the centrifuge test showed that a proper drainage system functioned as an appropriate channel to discharge infiltrating water quickly. For Case I without a drainage layer, the water that infiltrated through cracks in the dam continuously raised the water table inside the dam body. In contrast, for CASE

II with Zone 3Bs, the water table converged to a certain level corresponding to the drainage layer, thus representing a drainage system that can guarantee the safety of a CFGD in terms of seepage stability.

The amount of seepage flow is controlled by Zone 2 - underlying the concrete slab - whose hydraulic conductivity is much lower than that of other material zones. Thus, it is crucial to control the hydraulic conductivity of Zone 2 to limit the amount of seepage that infiltrates into the dam body. However, the centrifuge tests revealed the possibility that construction joints can undermine the original function of Zone 2, emphasizing the importance of quality control during the construction process as well as the design of a secondary seepage control mechanism in the form of an internal drainage zone.

The present study represents an initial attempt to understand the seepage behavior of a CFGD and the effectiveness of a drainage zone on seepage stability. Therefore, extensive future studies are required in order to fully utilize sand and gravel as construction materials in CFRDs.

Acknowledgements

The authors would like to thank GS Engineering & Construction Corp. and Korea Water Resources Corporation for funding this study and their efforts to collect valuable data. The authors also acknowledge all of the students and colleagues who worked with the KOCED Geotechnical Centrifuge Center at KAIST for their help in conducting the tests presented in this paper.

References

- Aubertin, M., Mbonimpa, M., Bussière, B., and Chapuis, R. P. (2003). "A model to predict the water retention curve from basic geotechnical properties." *Canadian Geotechnical Journal*, Vol. 40, No. 6, pp. 1104-1122.
- Chen, Q. and Zhang, L. M. (2006). "Three-dimensional analysis of water infiltration into the Gouhou rockfill dam using saturated-unsaturated seepage theory." *Canadian Geotechnical Journal*, Vol. 43, No. 5, pp. 449-461.
- Clements, R. P. (1984). "Post-construction deformation of rockfill dams." *Journal of Geotechnical Engineering*, ASCE, Vol. 110, No. 7, pp. 821-840.
- Cooke, J. B. (1984). "Progress in rockfill dams (18th Terzaghi Lecture)." *J. Geotechnical Engineering*, ASCE, Vol. 110, No. 10, pp. 1381-1414.
- Fredlund, D. G., Xing, A., and Huang, S. (1994). "Predicting the permeability function for unsaturated soils using the soil-water characteristic curve." *Canadian Geotechnical Journal*, Vol. 31, No. 4, pp. 533-546.
- Hunter, G. and Fell, R. (2003). "Rockfill modulus and settlement of concrete face rockfill dams." *Journal of Geotechnical and Geoenvironmental Engineering*, ASCE, Vol. 129, No.10, pp. 909-917.
- Kim, D. S., Kim, N. R., Choo, Y. W., and Cho, G. C. (2013). "A newly developed state-of-the-art geotechnical centrifuge in Korea." *KSCE Journal of Civil Engineering*, Vol. 17, No. 1, pp. 77-84.
- Liu, J. and Miao, L. J. (1996). "Experimental study of seepage and seepage stability of Gouhou rockfill materials." In *Gouhou Concrete-faced Rockfill Dam-design, Construction, Operation and Failure*, Ed. by China National Flood and Drought Prevention Office, Water Conservancy and Hydropower Press, Beijing, China, pp. 111-245.
- Pinto, N. L. S. (2008). "Very high CFRDs: Behaviour and design features." *International Journal on Hydropower and Dams*, Vol. 15, No. 4, pp. 43-49.
- Schofield, A. N. (1980). "Cambridge university geotechnical centrifuge operation, Rankine lecture." *Geotechnique*, Vol. 30, No. 3, pp. 227-268.
- Seo, M. W., Ha, I. S., Kim, Y. S., and Olson, S. M. (2009). "Behavior of concrete-faced rockfill dams during initial impoundment." *Journal of Geotechnical and Geoenvironmental Engineering*, ASCE, Vol. 135, No. 8, pp. 1070-1081.
- Taylor, R. N. (1995). "Centrifuge in modeling: Principles and scale effects." *Geotechnical Centrifuge Technology*, Blackie Academic and Professional, Glasgow, UK, pp. 19-33.
- Wang, Y. and Qu, L. (2000). "Design principle and method of seepage control of WULUWATI high concrete faced sandy gravel rockfill dam." *International Symposium on Concrete Faced Rockfill Dams (CFRD 2000)*, Beijing, China, pp. 425-437.
- Xavier, L. V., Albertoni, S. C., Pereira, R. F., and Antunes, J. (2008). "Behaviour and treatment of Campos Novos dam during second impounding." *International Journal on Hydropower and Dams*, Vol. 15, No. 4, pp. 53-58.
- Xing, H. F., Gong, X. N., Zhou, X. G., and Fu, H. F. (2006). "Construction of concrete faced rockfill dams with weak rocks." *Journal of Geotechnical and Geoenvironmental Engineering*, ASCE, Vol. 132, No.6, pp. 778-785.
- Xu, Z., Hou, Y. J., Liang, J., and Han, L. (2006). "Centrifuge modeling of concrete faced rockfill dam built on deep alluvium." *Proceedings of 6th International Conference Physical Modeling in Geotechnics*, Ng, Zhang, and Wang, Eds., Taylor & Francis Group, London, pp. 435-440.
- Zhang, L. M. and Chen, Q. (2006). "Seepage failure mechanism of the Gouhou rockfill dam during reservoir water infiltration." *Soil and Foundations*, Vol. 46, No. 5, pp. 557-568.